Improved Drag Element for Wind Tunnel Sting Balances

M. Ringel* and D. Levin†
Technion—Israel Institute of Technology, Haifa, Israel

In designing an internal sting balance, the main problems are encountered with drag element design. The adverse relation between sensitivity and stiffness leads to solutions with high nonlinear interactions. This paper presents a solution with minimized nonlinear interactions. The calibration results show an improvement of an order of magnitude in the linearity of the normal force interaction, and a better than 60% improvement in the linearity of the moment interaction. The new design enables a higher sensitivity level of the drag output with increased overall stiffness to be obtained. A new type of high resistance strain gage is presented after performing satisfactorily.

Nomenclature

a,h = distance in Fig. 3
d = output of drag element, μV
D = drag force
E = modulus of elasticity
i_d = interaction of output of the drag bridge
I = stiffness (moment of inertia)
M = pitching moment
N = normal force
$S_t D_v$ = standard deviation
V = voltage
α = deflection angle
δ = deflection
ϵ = strain

Introduction

AERODYNAMIC forces and moments acting on a model in small wind tunnels are often being measured by means of an integral internal sting balance. A balance consists of a mechanical component (Fig. 1) machined out of a solid high-strength steel bar, and an electrical circuitry (Fig. 2) consisting of strain gages and wiring. An integral strain-gage balance is required to be accurate, sensitive, structurally rigid, and with a low level of interaction between components. These properties tend to conflict, particularly in the case of small-diameter balances that are subjected to high loads.

In order to achieve these properties, complex design and manufacturing processes are applied. References 1-8 provide details of design and use of sting balances.

The most severe problems are encountered in the design of the drag, or axial force, measuring element of small-diameter balances. The high level of interaction, especially nonlinear interaction, of this element is almost inherent.

In general, interaction output is due to two sources. The first source is related to strain-gage techniques, and the second to the structural mechanism of the axial force element.

Strain-gage techniques and methods for electrical and mechanical compensations have been presented by White[9] and Seginer et al.[10] Improved results are obtained by using new types of self-temperature-compensated (STC) strain gages, as will be demonstrated later.

The second group of interactions is related to the structural mechanism and the combined nature of the aerodynamical loading. The main constituents of this group are as follows:

1) Machining inaccuracy.
2) Reorientation of loads due to balance deflection.
3) Deflection of the main beams of the drag element.
4) Additional deflection of the drag flexures due to combined loads.

While machining inaccuracy can be reduced by careful design and machining, reorientation of the loads is an inherent interaction. This situation is illustrated in Fig. 3. It is evident that the interaction is proportional to N^2/I, i.e., a nonlinear interaction. The only way to reduce this interaction is by increasing the stiffness I, i.e., a larger diameter.

In Fig. 4, a conventional axial force (drag) element is presented. The main beams, A and B, carry the loads in the pitch and yaw planes, as well as the rolling moment. These loads cause the beams to deflect. This deflection causes stresses in the drag element flexures, which are reflected as strains and output in drag gages. The reduction of this interaction can be achieved by enlarging the stiffness of the main beams, i.e., larger balance diameter.

In Fig. 5 an additional interaction is illustrated. This interaction occurs while combined axial normal loads are being applied. The axial force acting on the drag flexure causes a deflection δD. An additional deflection is caused by a normal force N being applied simultaneously. This interaction is of a nonlinear nature. Reduction of this interaction can be achieved by increasing the stiffness of the drag element flexures at the expense of reduced sensitivity.

Existing techniques for interaction compensation are based on the calibration process. In linear calibration, the linear interactions are compensated by using a 6×6 derivatives matrix (3 forces and 3 moments) to obtain wind tunnel loads. Although the linear calibration is simple to perform, it is sometimes not sufficiently accurate since it does not provide for nonlinear interactions. This leads to nonlinear calibration which deals with the nonlinear interactions by using a 6×27 matrix, as shown by Smith.[11] Nonlinear calibration is complicated both by finding the 6×27 derivatives and by using an iterative solution for wind tunnel loads.

Calibration and data processing permit making allowance for interactions, as long as the nonlinearity is substantially small. A new design of an axial force element is presented. This design is aimed at minimizing the last two nonlinear interactions.

Received Sept. 17, 1984; revision received July 1, 1985.

*Research Engineer.

†Head, Wind Tunnel Laboratory. Member AIAA.

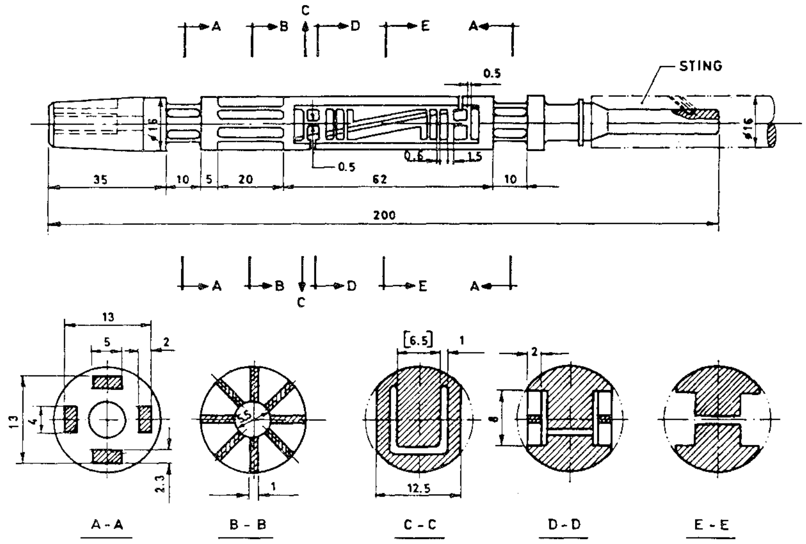

Fig. 1 Strain-gage balance 6452.

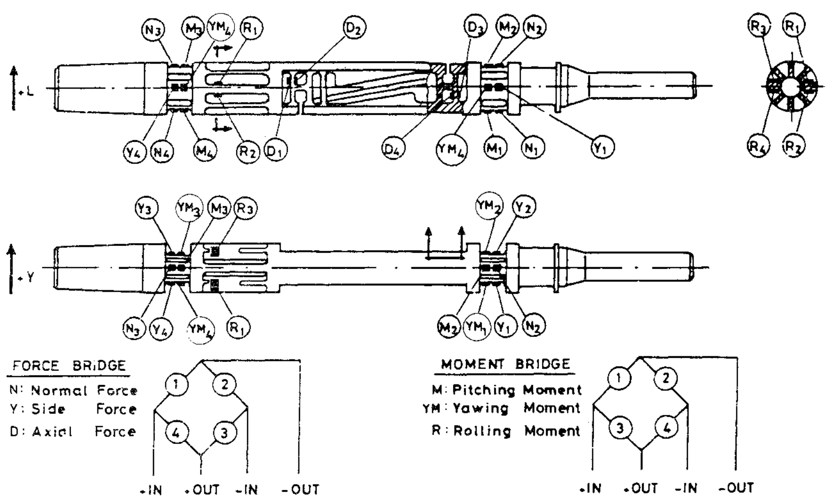

Fig. 2 Typical balance circuitry 6452.

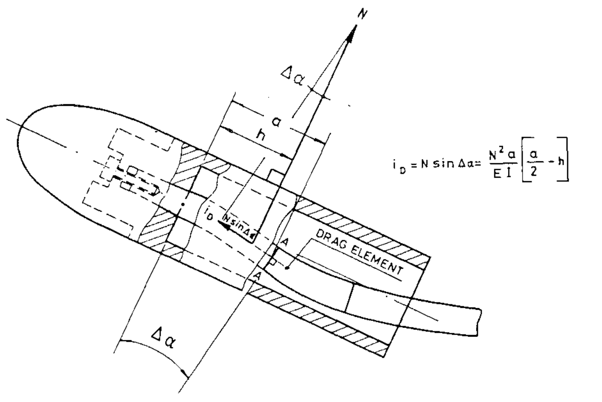

Fig. 3 Inherent lift interaction with drag (i_d).

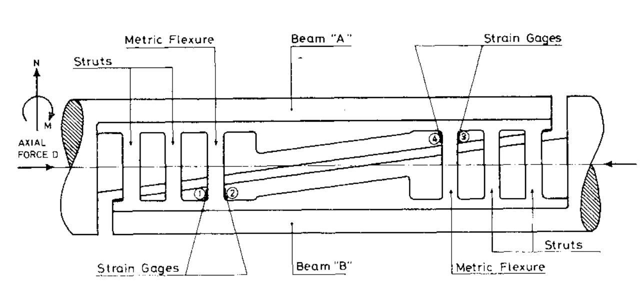

Fig. 4 Conventional drag element.

New Drag Element

A schematic illustration of the new drag element is shown in Fig. 6. The measured flexure does not carry the load directly, but follows the deflection of strut C.

The flexure undergoes two modes of deflection: axial and rotational. In the case of axial force action, a linear deflection takes place producing proportional output from the Wheatstone bridge (Fig. 7b). In case of loading in the pitch plane, axial and rotational deflection take place with no output of the drag bridge due to rotational deflection, Fig. 7c. In the case of combined loading, Fig. 8, a similar distinction between the axial (producing) and rotational (nonproducing) deflections will occur.

The new structure permits an increase of up to four times the stiffness of the drag struts without losing sensitivity. Since strain gages are not bonded to these struts and the need to achieve desired strain level for high sensitivity does not exist, this increased stiffness may reduce the nonlinearity at the drag element by an order of magnitude.

In addition, a new strain gase (FTKB2-S10075000) manufactured by Micro Measurements Group Inc. was introduced. This strain gage has a 5KΩ resistance, compared to 350Ω of the conventional type. This strain gage can support higher input voltage (18-36 V) in the Wheatstone bridge and thus be used to obtain higher sensitivity of the element without increasing hysteresis effects or overheating, and without decreasing the stiffness.

With the new drag element design and the new 5KΩ high-resistance strain gages with 18-V excitation, the drag element

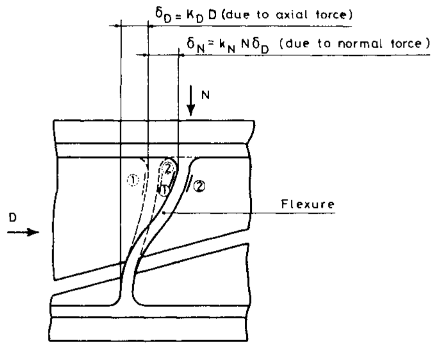

Fig. 5 Axial deflection combined with normal force (conventional drag element).

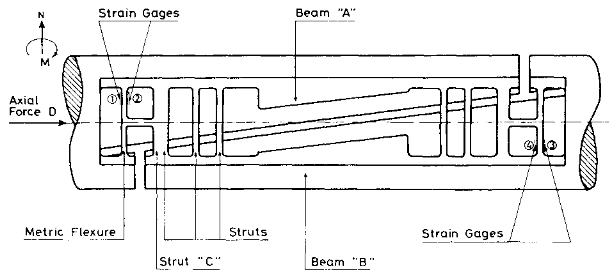

Fig. 6 Schematic of new drag element.

a) No loads.

b) Maximum output of the Wheatstone bridge with the flexure symmetrically bent, pure axial load.

c) Nominal zone output of the Wheatstone bridge with the flexure under pure asymmetric torque due to a normal force.

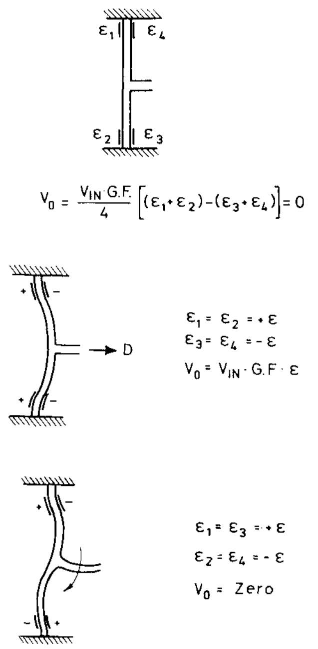

Fig. 7 Nominal output of the drag Wheatstone bridge with the metric flexure under pure axial and normal loads.

stiffness can be increased by more than 12 compared with the conventional drag element using 350Ω strain gages.

Results

A comparison test was conducted between two similar balances: balance 6452 (Fig. 2) with the new drag element ($I_{drag} = 2.5$ mm^4) and balance 6C28 with a conventional-type drag element ($I_{drag} = 2$ mm^4). The drag elements of the two balances were of similar stiffness, in order to observe the behavior of the new structure. The output of the two drag elements for normal force and pitching moment loading is

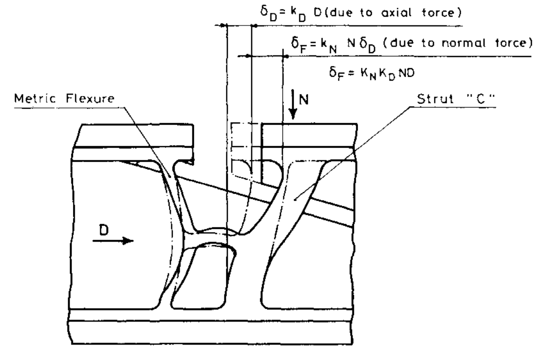

Fig. 8 Deflections under combined axial and normal forces.

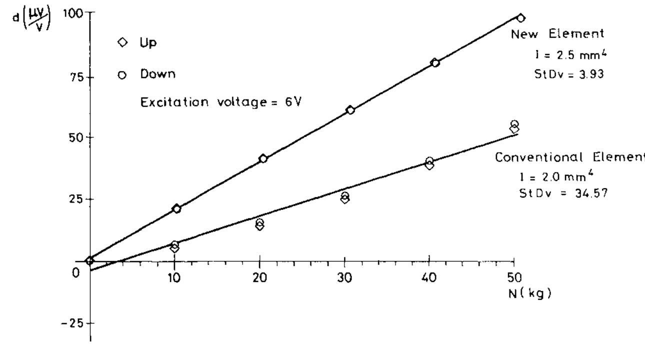

Fig. 9 Parasitic drag output under normal force.

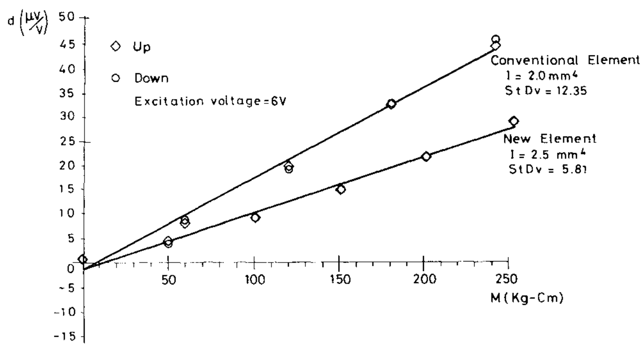

Fig. 10 Parasitic drag output under pitching moment.

compared in Figs. 9 and 10. Both balances had the same excitation voltage, 6 V.

The interaction of the normal force is shown in Fig. 9. The nonlinear part of the interaction is expressed by the standard deviation (S_tD_v) from the linear curve. It is evident that the improvement in this term is large, by an order of magnitude, and that the curve is practically linear.

Although complete linearity of the pitching moment coefficient has not been achieved (Fig. 10) an improvement of better than 60% was obtained.

Conclusion

The new drag element has reduced the nonlinearity of the normal force interaction by an order of magnitude, making it linear for all purposes. The nonlinearity of the pitching moment interaction has been reduced considerably. These results have been obtained without reducing the balance sensitivity and with increasing the balance stiffness by only 25%.

The new drag element design may prove valuable for the design of small-diameter balances, the stiffness of which is limited, in order to obtain measurable output.

Another primary gain is that the stiffness of the drag struts may be increased by more than 400% without impairing the sensitivity of the drag output.

A new type of high-resistance strain gage has been used successfully. It has demonstrated the practicability of a Wheatstone bridge with high input voltage and, thus, higher output with no mechanical change in the measuring element. With 18-V excitation, balance sensitivity was increased by 300% compared with conventional 350Ω strain gages. This output did not suffer from increased hysteresis or overheating.

An overall improvement of better than 12 times in sensitivity or stiffness was achieved by the new drag element structure and by the use of new high-resistance strain gages.

References

[1]Moss, G. F. and Payne, D. G., "A Compact Design of a Six Component Internal Strain Gauge Balance," Royal Aeronautical Establishment, Bedford, U. K., TN AERO 2764, July 1961.

[2]Pope, A. and Goin, K. L., *High Speed Wind Tunnel Testing*, John Wiley and Sons, New York, 1965, pp. 242-283.

[3]Hansen, R. M., "Mechanical Design and Fabrication of Strain Gauge Balances," AGARD Rept. 9, Feb. 1965.

[4]Dubois, M., "Fabrication of High Precision Strain Dynamometers and Balances at the ONERA Modane Center," ONERA, TP 1196, Feb. 1973.

[5]Dubois, M., "Calibration of Six-Component Dynamometric Balances," ONERA TP 1976-79, May 1976.

[6]Heyser, A., "Entwicklung von Windkanaleinbauwaagen mit Dehnungsmesstreifensystemen," DFVLR, Proz-Wahn Bericht, No. 261, May 1963.

[7]Rebuffet, P., "Some Strain Gauge Balances used in French Wind Tunnels," ONERA, TN 31, Feb. 1956.

[8]Gorlin, S. M. and Slezinger, I. I., "Wind Tunnels and Their Instrumentation," (translated from Russian), *Israel Program for Scientific Translations*, Jerusalem, 1966, pp. 379-425.

[9]White, G., "Temperature Compensation of Bridge Type Transducers," *Statham Instrument Notes*, No. 5, Oct.-Nov. 1948, revised Aug. 1951.

[10]Seginer, A., Brosh, A., and Richard, R. D., "A Parametric Investigation of an Elastic Parallelogram for the Measurement of Aerodynamic Drag," Technion—Israel Institute of Technology, Haifa, Israel, TAE Rept. 419, July 1980.

[11]Smith, D. L., "An Efficient Algorithm Using Matrix Methods to Solve Wind-Tunnel Force-Balance Equations," NASA TN D-6860, Aug. 1972.